

Phased Array Antennas for MMwave Applications

¹Matta Venkata Durga Pavan Kumar, ²Mamatha B, ³Akkiseti Vn Hanuman, ⁴Rayudu Vinay Kumar

Submitted: 07/09/2024 Revised: 20/10/2024 Accepted: 29/10/2024

Abstract: The beam-steering antenna is crucial and extensively used in communication systems. This communication presents the design of a 28 GHz beam-steering phased array antenna for 5G millimeter-wave applications. The aim of this project is to examine and deploy a phase shifter in a linear antenna array for angular scanning. The proposed array antenna has four microstrip patch antenna components, with each feed port coupled to a phase shifter. The primary mechanism of radiation arises from the activation of elements in succession with varying phase delays. The emitted beam may be directed in various orientations based on the initial excitation of the components. In the first instance, three-dimensional radiation is emitted at a 0° phase. The second configuration achieves commendable scanning performance throughout a range of $\pm 10^\circ$ to $\pm 40^\circ$, with an acceptable side lobe level and a gain of 12.1 dB.

Keywords: Linear Array; Phase Shifters; Phased Array; Radiation Pattern; Microstrip Antenna; Beam Direction.

INTRODUCTION

This article identifies millimeter-wave communication as a crucial facilitator for 5G applications.

Phased array antennas may assume several configurations, including linear, planar, and circular. Phased array antennas are mostly used to electrically direct the main beam (main lobe, broadside) of the antenna. It functions by postponing signals emitted by antenna elements via the use of phase shifters on each element. This results in constructive and destructive interference, hence causing the beam to deviate from the nominal direction of a single antenna element [1],[6].

This study examines linear phased array antennas composed of unit cells, each consisting of radiating components powered by transmit and receive modules capable of amplitude and phase modulation. Linear phased arrays use progressive phase stimulation among the components to electronically scan the antenna beam in one dimension. The primary benefits of phased arrays compared to traditional systems are enhanced scanning speed, superior dependability, and multifunctional capabilities. These benefits make the adoption of this technology the most rational option for the next generation of weather radars.

This study is primarily motivated by the use of linear active phased arrays in future low-cost weather radars; hence, this research aims to elucidate the fundamental principles pertaining to the theory of linear phase arrays and their applicability in antenna design.

principle. Section III addresses concerns pertaining to the suggested patch antenna design and its simulation outcomes. Section IV delineates the suggested structure of the phased array antenna, followed by the conclusion.

5G communications at mmWaves frequency bands give additional important radio spectrum for wireless communications [1–3]. This is in response to the exponential rise of wireless data transfer applications in a variety of scenarios. The huge bandwidth that is available for use in millimeter-wave communications has the potential to significantly boost the speed at which wireless data may be sent in a variety of applications [4–6]. Particularly noteworthy is the fact that the Federal Communications Commission (FCC) of the United States has not only made a significant amount of spectrum accessible in the 28–73 GHz band, but it is also conducting a study of the bands that will be available in the future [7–9]. As a result, mmWave has a tremendous deal of potential for both study and application. However, the high propagation loss and the poor signal-to-noise ratio (SNR) at mmWave frequencies have hindered the fast spread of mmWave communications to a substantial degree

^{1,2,3,4}International School of Technology and Sciences for Women, A.P, India.

[10,11].

directional high gain antennas are frequently utilized as system transmitters (Tx) or receivers (Rx) in communication systems [12–14]. This is done in order to overcome the disadvantages of millimeter wave (mmWave) that have been stated above and to expand the range of mmWave radio transmission. However, when the gain of the antenna grows, the beam-width of the antenna drops, which results in a reduction in the effective coverage that the antenna provides. The significance of beam-tracking cannot be overstated when it comes to ensuring reliable communication in dynamic settings where the positions of Tx/Rx and propagation circumstances are subject to change over time. Furthermore, in order to provide real-time tracking of the prevailing propagation routes, electrical beam-steering of phased arrays is a crucial component [15–17]. An antenna, a phase shifter, and an attenuator are the three components that make up each radio frequency chain in mmWave systems, which are why phased array systems are so extensively utilized in these systems [18]. It is possible to customize the phase and amplitude excitation of each element with the assistance of phase shifters and attenuators. This has the effect of allowing the phased array beam pattern to be guided to certain spatial directions.

All of the antennas and control circuits that are characteristic of a phased array system are included into a single package by an AiP system. This makes it possible to have minimal expenses for development and maintenance, rapid product iterations, simple installation and mobility, and low energy usage for operational purposes inside the system. Radios, automobile radars, and image sensors are just some of the applications that have made extensive use of AiP technology in the mmWave sector [19–21]. The primary hardware and control architecture of an 8×8 AiP that is expanded based on the 4×4 AiP design architecture published in [22] are provided in this work after being extended. Before the implementation of the AiP, a number of tests are carried out in order to validate the stability of the AiP and assess the precision of the elemental composite weight control. In addition, two examples of applications of the AiP are shown, in which the AiP is used as an experimental platform for phased array calibration and mmWave channel sounding, respectively. These examples are outlined below:

Setting the complex weight for each element in a phased array system in the appropriate manner is

what is required to accomplish beamforming. Because of this, it is very necessary to calibrate out the initial excitations of the array members in order to ensure that the beamforming performance is satisfactory. [23–26] The literature has a variety of different calibration techniques that have been suggested, specifically for frequency bands that are below 6 GHz. Within the scope of this study, our objective is to explore the effectiveness of the calibration approach in the context of realistic mmWave phased arrays. To be more precise, we would want to explore (1) the degree to which the AiP is stable in its operation and (2) the degree to which the temperature of the AiP influences the accuracy of the array calibration. The third question is how much the calibration can assist enhance the beamforming performance, and the fourth question is how precise array calibration the various calibration techniques can accomplish in real mmWave AiPs.

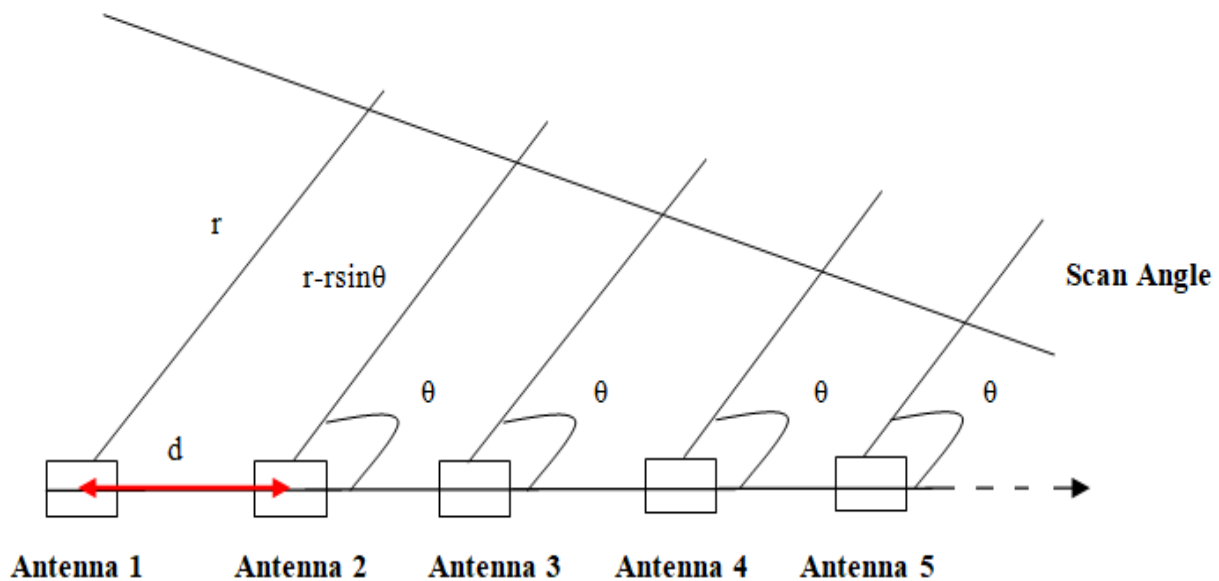
PHASED ARRAY ANTENNA

In a single-element antenna, the radiation pattern is typically wide, and the directivity is comparatively low. The issue may be influenced by increasing the size of the element, hence enhancing directivity. One method to augment the antenna without altering the dimensions of the individual components is to arrange the radiating elements in a geometric arrangement referred to as a "array" [5]. The components of the array are typically uniform and may take many forms (e.g., wire antennas, microstrip patches, etc.). Numerous antenna system applications need the temporal alteration or scanning of the beam's principal lobe direction. This is often accomplished by mechanically rotating a single antenna or an array with a fixed phase relative to the elements. Nonetheless, mechanical scanning necessitates a positioning system that might be expensive and operates at a sluggish pace. Consequently, electronic scanning antennas, referred to as phased array antennas, are used. The beam's direction may be altered by electronically adjusting the phase of the radiating element, so creating a dynamic pattern without any mechanical movement. Phased array antennas are recognized for their ability to electronically steer the beam pattern with great efficiency, achieving minimal side-lobe levels and narrow beamwidth. To attain performance standards like narrow beamwidth or extensive scanning range with high angular precision, a substantial quantity of antenna

components was required to assemble the array. Phase shifters are typically the components of a

phased array antenna that enable the steering of the emitted beam in a certain direction.

Phase front



In Figure 1. shows a uniform linear array of N equally spaced elements having a grating step (separating two adjacent antennas). These sources are fed with the same amplitude and with a phase gradient $\Delta\phi$ with respect to each other. r represents the maximum distance between the reference antenna and the observation plane, and θ is the beam steering angle.

PROPOSED ANTENNA

The suggested single-patch antenna structures are shown in Figure 2, which displays their geometrical layout. consists of a typical square patch that is supplied with the transmission line structure before being printed on a Rogers RT/Duroid5880 substrate. This substrate has a permittivity of 2.2, a loss tangent of 0.001, and a thickness of $h = 0.25\text{mm}$. The suggested antenna spans a surface area of 10 millimeters by 15 millimeters, and its dimensions have been computed and tuned to ensure that it resonates at a frequency of 28 gigahertz. The suggested antenna has the following final dimensions: $L_p=W_p= 3.36\text{mm}$, and the frequency is determined by applying patch antenna equations.

$L_q= 2\text{mm}$, $W_q= 0.145\text{mm}$, $L_f = 3\text{mm}$ and $W_f = 0.776\text{mm}$.

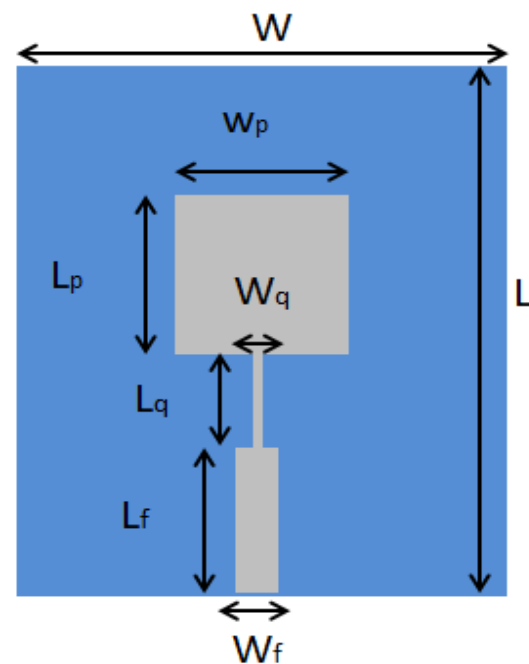


Fig. 2. Geometry of the proposed patch antenna.

Both oblation and inferior gain are included. On the other hand, there are secondary lobes that have a large gain and are regarded as parasitic radiation. It is necessary to get the antennas as close together as possible in order to lower the level of the side lobes. It is vital to note that the field to antenna coupling is more significant the closer they are to one another. The decrease of the side lobe level necessitated the need to establish a compromise between the separation distance and the coupling between

antennas. This was essential because it was important to find a compromise. In light of this study, we determined that a separation distance of 0.5λ would be the most ideal choice. This is due to the fact that the array has favorable performance characteristics at the side lobes level, coupling between antennas, and gain of antenna.

4 Linear array antenna

Phased array antennas are well-known for their capacity to electronically steer the beam pattern with a high degree of efficiency, hence achieving narrow beamwidths and side-lobe levels that are as low as possible. Typically, phase shifters are the components of a phased array antenna that are responsible for directing the emitted beam in the desired direction [4]. The purpose of this section is to study a phase shifter that is included into a linear antenna array for the purpose of angle scanning. Figure 6 illustrates a linear array consisting of four elements. Each element is stimulated with an equal amplitude and a progressive phase shift $\Delta\phi$, which is defined by the element's position within the array.

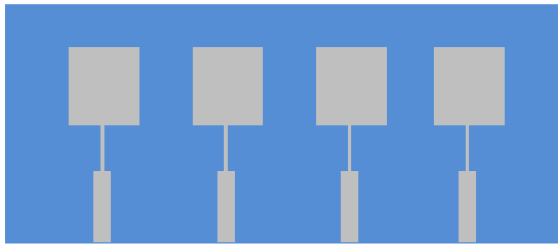
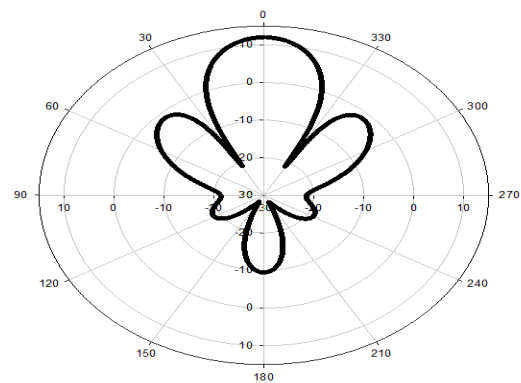


Fig. 3. Array of four element microstrip patch.

A representation of the antenna's return loss may be seen in Figure 7. According to the findings, the resonance frequency of the antenna is 28.03 GHz, and the ratio of S11 to S22 is -16.17 dB, while the ratio of S33 to S44 is -14.78 dB. Two point three percent is the bandwidth of the antenna.

In the first place, all of the ports are activated by 0 phase and equal amplitude. Figure 8 displays the results of the radiation patterns in the (XY) E-plane, as well as attributes such as beam location, maximum gain, and SLL. There is a maximum gain of 12 decibels in broadside ($\theta=0^\circ$) orientation. At the E-plane, the SLL is equivalent to -13.5 decibels in this case. In the second phase, in order to investigate the beam scanning capabilities of the array antenna,

each of the ports is stimulated by a scanning that is more than $\pm 40^\circ$ and has an identical amplitude. As illustrated in Figure 9, the radiation pattern for the (XY) E-plane is shown for a variety of phase values ranging from -40 degrees to 40 degrees at a resonance frequency of 28 gigahertz. Although the gain for all scans is 12 dB, the side lobe level is -10.8 dB when the beam is slanted by $\pm 30^\circ$ and $\pm 40^\circ$. However, the gain stays the same at 12 dB regardless of the tilt. At a frequency of 28 GHz, the beam tilting of $\pm 20^\circ$ results in a signal-to-noise ratio (SLL) of -11.5 dB, while the beamwidth is 26.3° .



Mmwave Channel Sounding

The four-in-four AiP described in [22] is used as the transmitter in a mmWave channel sounder, which is yet another application of the AiP. Figure 12 illustrates the overall environment and the configuration of the system that was used for the AiPs channel sounding measurement. The metal plate is purposefully inserted into the channel environment in order to perform the function of a reflector with the objective of producing a reflection route.

Figure 5 depicts the precise positioning of the Tx, the Rx, and the metal plate relative to the floor. The Tx and Rx are both positioned at a height of 1.2 meters above the ground. It is linked to the Tx port of the VNA, while port 2 is connected to the Rx port. By measuring the S-parameter with the VNA, one may determine the channel frequency response that exists between the Tx and the Rx. In order to regulate the transmission, laptop 1 is used, while laptop 2 is in charge of regulating the transmission and the VNA.

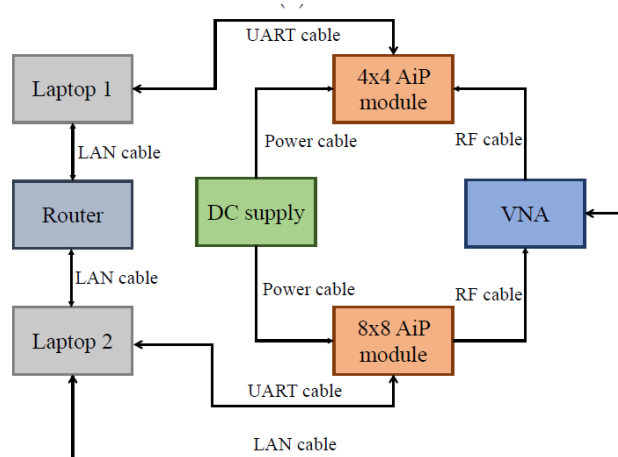


Figure 5: Block diagram of the AiPs channel sounder setup

In order to facilitate the connection between laptop 1 and laptop 2, as well as between laptop 2 and the VNA, which is physically linked by a LAN cable, the router serves as a relay. The TCP/IP protocol is used to communicate between laptop 1 and laptop 2, whereas the SCPI protocol is used to connect between laptop 2 and the virtual network adapter (VNA). In order to communicate via the Serial Communication protocol, the AiPs are linked to the laptops through the use of UART connections. At the time when the AiPs channel sounder is taking measurements of the channel, laptop 1 is in charge of controlling the Tx AiP beam-steering. This allows the AiP to beam-steer from 53 degrees to 53 degrees in the horizontal plane. Laptop 2 is responsible for controlling the Rx AiP guiding beams in the horizontal plane from a range of -72 degrees to 72 degrees for each beam that is directed by the Tx AiP.

Furthermore, laptop 2 is also responsible for controlling the VNA, which ensures that the frequency response between the Tx and Rx is recorded.

CONCLUSION

An investigation of a phased array structure has been presented and discussed in this article. In order to perform beam steering, phase shifters are used in the formation of the structure, which is constructed by evenly arranging as a four-element identical. A change in the phase of the element is what is required to accomplish the phase shift. This final suggested antenna is capable of achieving a bandwidth of 750 MHz for S11, which is less than -10 dB. It is designed to span the frequency range of

27.74-28.31 GHz, which is planned for future millimeter wave communications. In addition, the antenna array was able to attain a maximum gain of 12 dB in the broadside direction. One possible use of the antenna array is as a phased array, which would allow it to be deployed for the purpose of directing the radiation beam. The antenna had a very nice radiation pattern and a gain that was consistent throughout. An antenna may shift its beams between 0 degrees, ± 10 degrees, ± 20 degrees, ± 30 degrees, and ± 40 degrees in the xoy plane at 28 GHz. This is because the structure can have nine different types of reflection phase distribution. Additionally, in comparison to previous beam steering antennas, the suggested antenna is capable of achieving a greater beam tilting angle of forty degrees. The subsequent stage is to proceed with the fabrication of the antenna and the verification of the simulation findings, which will be presented at the conference.

REFERENCES

- [1] D. Ehyae: Novel Approaches to the Design of Phased Array Antennas. pp. 1-11 2011.
- [2] T. Eray, H. Jurgén, W. Christoph, Z. Thomas: A novel millimeter-wave dual-fed phased array for beam steering. IEEE transaction on microwave theory and technique. Vol. 61, pp. 40-43. 2013.
- [3] M. Dorra: Etude comportementale et conception d'un réseau d'oscillateurs couplés intégré en technologie silicium appliqué à la commande d'un réseau d'antennes linéaire. 2013.

- [4] L. Jinxin, Z. Qingsheng, L. Ruizhi, A. Tayeb: Beam-tilting antenna with negative refractive index metamaterial loading. *IEEE antennas and wireless propagation letters*. Vol. 61, pp. 40-43. 2017.
- [5] Y. Yazid, G. Xun: A low-cost patch antenna phased array with analog beam steering using mutual coupling and reactive loading. *IEEE antenna and wireless propagation letters*. Vol. 7. 2012.
- [6] M. Khalily, R. Tafazolli, T. A. Rahman, and M. R. Kamarudin: Design of phased arrays of series-fed patch antennas with reduced number of the controllers for 28 GHz mm-wave applications. *IEEE Antennas and Wireless Propagation Letters*, vol. 15, pp. 1305–1308, 2016.
- [7] T. Eray, H. Jurgen, W. Christoph, Z. Thomas: Reconfigurable Beam Steering Using a Microstrip Patch Antenna With a U-Slot for Wearable Fabric Applications. *IEEE antennas and wireless propagation letters*. Vol. 15, 2013.
- [8] L. Teng, Z. N. Chen: Control of Beam Direction for Substrate-Integrated Waveguide Slot Array Antenna Using Metasurface. *IEEE Transaction On Antennas And Propagation*. 2018.
- [9] R. Badreddine, L. Andre, P. Gerard, N. Shah: Modeling and design of metasurfaces for beam scanning. *Appl. Phys. Lett.* 50, 123, 2017.
- [10] Gu, X.; Liu, D.; Baks, C.; Tageman, O.; Sadhu, B.; Hallin, J.; Rexberg, L.; Parida, P.; Kwark, Y.; Valdes-Garcia, A. Development,
- [11] Implementation, and Characterization of a 64-Element Dual-Polarized Phased-Array Antenna Module for 28-GHz High-Speed
- [12] Data Communications. *IEEE Trans. Microw. Theory Tech.* **2019**, 67, 2975–2984.
- [13] 17. Wang, Y.; Chung, H.; Ma, Q.; Rebeiz, G.M. A 57.5–65.5 GHz Phased-Array Transmit Beamformer in 45 nm CMOS SOI With 5
- [14] dBm and 6.1 Linear PAE for 400 MBaud 64-QAM Waveforms. *IEEE Trans. Microw. Theory Tech.* **2021**, 69, 1772–1779.
- [15] 18. Herd, J.S.; Conway, M.D. The Evolution to Modern Phased Array Architectures. *Proc. IEEE* **2016**, 104, 519–529.
- [16] 19. Zhang, Y.P.; Liu, D. Antenna-on-Chip and Antenna-in-Package Solutions to Highly Integrated Millimeter-Wave Devices for
- [17] Wireless Communications. *IEEE Trans. Antennas Propag.* **2009**, 57, 2830–2841.
- [18] 20. Zhang, Y.; Mao, J. An Overview of the Development of Antenna-in-Package Technology for Highly Integrated Wireless Devices.
- [19] *Proc. IEEE* **2019**, 107, 2265–2280.
- [20] 21. Zwenger, C.; Chaudhry, V. Antenna in package (AiP) technology for 5G growth. *Chip Scale Rev.* March/April **2020**, 351. Available
- [21] online: https://www.chipscalereview.com/wp-content/uploads/2021/01/ChipScale_Mar-Apr_2020-wp.pdf (accessed on 28
- [22] November 2022).
- [23] 22. Gao, H.; Wang, W.; Fan, W.; Zhang, F.; Wang, Z.; Wu, Y.; Liu, Y.; Pedersen, G.F. Design and Experimental Validation of Automated
- [24] Millimeter-Wave phased Array Antenna-in-Package (AiP) Experimental Platform. *IEEE Trans. Instrum. Meas.* **2021**, 70, 1–11.
- [25] 23. Zhang, F.; Fan, W.; Wang, Z.; Zhang, Y.; Pedersen, G.F. Improved Over-the-Air Phased Array Calibration Based on Measured
- [26] Complex Array Signals. *IEEE Antennas Wirel. Propag. Lett.* **2019**, 18, 1174–1178.
- [27] 24. Seiji, M.; Katagi, T. A method for measuring amplitude and phase of each radiating element of a phased array antenna. *Electron.*
- [28] *Commun. Jpn. Part Commun.* **1982**, J65-B, 555–560.
- [29] 25. Takahashi, T.; Konishi, Y.; Chiba, I. A Novel Amplitude-Only Measurement Method to Determine Element Fields in Phased
- [30] Arrays. *IEEE Trans. Antennas Propag.* **2012**, 60, 3222–3230.
- [31] 26. Long, R.; Ouyang, J.; Yang, F.; Han, W.; Zhou, L. Fast Amplitude-Only Measurement

Method for Phased Array Calibration. IEEE

- [32]Trans. Antennas Propag. **2017**, 65, 1815–1822.
- [33]27. Hejselbæk, J.; Nielsen, J.; Fan, W.; Pedersen, G.F. Measured 21.5 GHz Indoor Channels With User-Held Handset Antenna Array.
- [34]IEEE Trans. Antennas Propag. **2017**, 65, 6574–6583.
- [35]28. Mbugua, A.W.; Fan, W.; Olesen, K.; Cai, X.; Pedersen, G.F. Phase-Compensated Optical Fiber-Based Ultrawideband Channel
- [36]Sounder. IEEE Trans. Microw. Theory Tech. **2020**, 68, 636–647.
- [37]29. Zwick, T.; Beukema, T.; Nam, H. Wideband channel sounder with measurements and model for the 60 GHz indoor radio channel.IEEE Trans. Veh. Technol. **2005**, 54, 1266–1277.